Nanomed Res J 11(2):177-187, Spring 2026

RESEARCH ARTICLE

Biogenic Silver Nanoparticles Synthesized from *Rhamnus persica* Induce Apoptosis and Transcriptional Changes in ECM-Associated Genes

Amir Mohammad Bayat, Mahsa Kavousi*

Department of Biology, ET.C., Islamic Azad University, Tehran, Iran

ARTICLE INFO

Article History:
Received: 2025-11-17
Revised: 2026-02-05
Accepted: 2026-02-15

Keywords:
Green Synthesis
Cytotoxicity
Caspase Activation
Apoptosis
Nanobiotechnology
Phytochemicals

ABSTRACT

Triple-negative breast cancer (TNBC) is one of the most aggressive breast cancer subtypes and is associated with limited therapeutic options and poor clinical outcomes. The development of green nanotechnology-based delivery systems has emerged as a promising strategy to enhance the biological performance of plant-derived bioactive compounds. In the present study, silver nanoparticles (AgNPs) were biosynthesized from Rhamnus persica leaf extract using an environmentally friendly precipitation approach and characterized by UV–Vis spectroscopy, X-ray diffraction (XRD), Fourier transform infrared (FTIR) spectroscopy, dynamic light scattering (DLS), and electron microscopy.

The biological activity of the synthesized AgNPs was investigated in MDA-MB-231 triple-negative breast cancer cells. Cell viability was determined using the MTT assay, apoptotic cell death was quantified by Annexin V-FITC/PI flow cytometry, and the transcriptional expression of apoptosis-related genes (Caspase-3 and Caspase-9) together with extracellular matrix-associated genes (MMP2 and MMP9) was analyzed by quantitative real-time PCR.

Compared with the crude plant extract, R. persica-mediated AgNPs demonstrated markedly enhanced cytotoxic activity, yielding an IC_{50} value of 9.45 µg/mL. Flow cytometric analysis confirmed a substantial increase in apoptotic cell populations following nanoparticle treatment, whereas only a limited proportion of cells underwent necrosis.

Gene expression analysis revealed significant transcriptional upregulation of Caspase-3 and Caspase-9 accompanied by reduced expression of MMP2 and MMP9. Because these measurements were confined to mRNA expression, they should be interpreted as molecular findings and not as evidence of functional changes in cell migration or invasion. Collectively, these results indicate that biosynthesized R. persica AgNPs enhance the cytotoxic and pro-apoptotic effects of the plant extract against TNBC cells while providing preliminary molecular evidence to support future mechanistic and translational investigations.

How to cite this article
Mohammad Bayat A, Kavousi M. Biogenic Silver Nanoparticles Synthesized from Rhamnus persica Induce Apoptosis and Transcriptional Changes in ECM-Associated Genes. Nanomed Res J, 2026; 11(2): 177-187. DOI: 10.22034/nmrj.2026.02.008

INTRODUCTION

Breast cancer continues to impose a substantial global health burden and remains one of the most frequently diagnosed malignancies among women. Despite remarkable advances in screening programs, diagnostic technologies, and therapeutic interventions, it is still responsible for considerable morbidity and mortality worldwide [1,2]. Among the recognized molecular subtypes, triple-negative breast cancer (TNBC) is regarded as one of the most clinically aggressive forms because of its unfavorable prognosis and limited therapeutic options [3,4]. The lack of estrogen receptor (ER), progesterone receptor (PR), and human epidermal growth factor receptor 2 (HER2) expression renders TNBC unresponsive to endocrine therapy and HER2-targeted agents, leaving systemic chemotherapy as the primary treatment strategy [5,6]. However, treatment efficacy is frequently compromised by

* Corresponding Author Email: *ma.kavousi@iau.ac.ir*

drug resistance, disease recurrence, and dose-limiting toxicities, highlighting the need for more effective and less toxic therapeutic alternatives [7,8].

Natural products have emerged as an important source of novel anticancer compounds, and medicinal plants continue to attract attention because of their rich repertoire of biologically active phytochemicals. Flavonoids, alkaloids, phenolic compounds, and related secondary metabolites have been reported to regulate multiple cellular signaling pathways involved in apoptosis, oxidative stress, cell proliferation, and other processes associated with tumor progression [9–12]. Their multitargeted mechanisms of action, together with their relatively favorable safety profiles, make plant-derived compounds promising candidates for the development of complementary or alternative anticancer therapies [13].

Among these medicinal plants, *Rhamnus persica*, a thorny shrub belonging to the Rhamnaceae family and native to Iran, has recently attracted increasing scientific interest. Traditionally, this species has been used for its laxative, anti-inflammatory, and detoxifying properties [14]. Phytochemical investigations have demonstrated that *R. persica* contains diverse bioactive constituents, including anthraquinones, flavonoids, and phenolic compounds, many of which have been associated with antioxidant and cytotoxic activities [15]. These phytochemicals may influence molecular pathways involved in cancer cell survival, apoptosis, and extracellular matrix regulation, suggesting that *R. persica* could represent a valuable source of anticancer agents [16,17].

Based on these considerations, the present study aimed to investigate the anticancer activity of biogenic silver nanoparticles synthesized using *R. persica* leaf extract against the MDA-MB-231 cell line, a widely used model of triple-negative breast cancer. In addition to evaluating cytotoxicity, the study combined apoptosis assessment with targeted transcriptional analysis of apoptosis-related genes (*Caspase-3* and *Caspase-9*) and extracellular matrix-associated genes (*MMP2* and *MMP9*) to provide preliminary molecular insight into the biological effects of the synthesized nanoparticles. The investigation was intentionally limited to cytotoxicity, apoptosis profiling, and gene expression analyses; therefore, functional assays related to cell migration, invasion, or metastatic behavior were not performed. Accordingly, the observed transcriptional changes should be interpreted as molecular findings rather than evidence of functional anti-metastatic activity. The novelty of this work resides in integrating green synthesis of *R. persica*-mediated silver nanoparticles with gene-level mechanistic evaluation in a triple-negative breast cancer model, thereby establishing a foundation for future functional and translational investigations.

MATERIALS AND METHODS

Plant Material and Extract Preparation

The aerial parts of *Rhamnus persica* were collected, air-dried, and ground into a fine powder before extraction. Ethanolic extracts were obtained by Soxhlet extraction using 10 g of powdered plant material in 100 mL of 70% ethanol. After filtration, the extracts were stored at 4°C until further use. For nanoparticle synthesis, an aqueous extract was prepared by heating the plant material in distilled water followed by filtration. The resulting filtrate served as the biological reducing and stabilizing agent for the green synthesis of silver nanoparticles in the presence of $AgNO_3$ and polyvinylpyrrolidone (PVP). Comprehensive phytochemical characterization, including HPLC or LC–MS analysis, was not performed because the objective of this investigation was to evaluate the extract as a natural reagent for nanoparticle biosynthesis rather than to isolate or identify its individual constituents.

Biosynthesis and Characterization of Silver Nanoparticles

Silver nanoparticles were synthesized using the aqueous leaf extract of *R. persica* through a green reduction approach. Briefly, 4 mL of the extract was added to a 1 mM silver nitrate solution and gently stirred at room temperature for 1 h. Successful nanoparticle formation was indicated by a visible color transition from pale yellow to dark brown, reflecting the reduction of Ag^+ ions. The synthesized nanoparticles were collected by centrifugation at 13,000 rpm for 15 min and washed repeatedly with distilled water to eliminate residual silver ions and plant-derived impurities. The purified pellet was subsequently dried at 37°C.

The physicochemical characteristics of the biosynthesized AgNPs were evaluated using multiple analytical techniques. Transmission electron microscopy (TEM) and scanning electron

microscopy (SEM) were employed to determine particle morphology and size distribution. Crystalline structure was examined by X-ray diffraction (XRD), while Fourier-transform infrared (FTIR) spectroscopy was used to identify functional groups involved in nanoparticle reduction and stabilization. FTIR spectra were processed using Origin software. Dynamic light scattering (DLS) analysis was performed to determine hydrodynamic diameter and polydispersity index, and UV–Visible spectroscopy was used to verify nanoparticle formation through surface plasmon resonance analysis.

Cell Culture

Human triple-negative breast cancer MDA-MB-231 cells were maintained in RPMI-1640 medium supplemented with 10% fetal bovine serum (FBS) and 1% penicillin–streptomycin under standard culture conditions (37°C in a humidified incubator containing 5% CO_2). Cells were subcultured after reaching approximately 80% confluence using Trypsin–EDTA, collected by centrifugation, and reseeded at appropriate densities for subsequent experiments. Fresh culture medium was supplied every 48 h or earlier when medium acidification indicated increased metabolic activity.

For long-term preservation, cell suspensions with viability exceeding 90% were cryopreserved in freezing medium consisting of 90% RPMI-1640 and 10% FBS. Samples were initially stored at –80°C before transfer to liquid nitrogen. Frozen cells were rapidly thawed, washed to remove cryoprotective medium, resuspended in fresh culture medium, and used for experiments after confirming viability with 0.4% Trypan Blue staining. All cell culture procedures were conducted under sterile conditions inside a laminar airflow cabinet following routine UV sterilization and ethanol disinfection.

Cytotoxicity Assay

The cytotoxic activity of the synthesized AgNPs was evaluated using the MTT colorimetric assay. MDA-MB-231 cells were seeded into 96-well plates at a density of 1×10^4 cells per well and allowed to attach before treatment. Cells were exposed to AgNP concentrations of 100, 50, 25, 12.5, 6.25, and 3.125 μg/mL for 24 h. Following treatment, MTT solution (0.5 mg/mL) was added to each well and incubated for 3 h to allow formazan crystal formation. The crystals were dissolved in dimethyl sulfoxide (DMSO), and absorbance was measured at 570 nm using a microplate reader.

Gene Expression Analysis

Total RNA was isolated from treated and untreated MDA-MB-231 cells and reverse-transcribed into complementary DNA (cDNA) according to the manufacturer's protocol. cDNA concentration and purity were determined using a NanoDrop spectrophotometer, and equal amounts of template were used in all amplification reactions. Quantitative real-time PCR was carried out using Bioneer Master Mix and gene-specific primers targeting *Caspase-3*, *Caspase-9*, *MMP2*, and *MMP9*, with β-actin serving as the internal reference gene. Each biological sample was analyzed in technical triplicate.

PCR amplification consisted of an initial denaturation step at 95°C for 10 min followed by 40 amplification cycles of 95°C for 20 s, 55°C for 20 s, and 72°C for 20 s. Threshold cycle (Ct) values

Table 1. Primer sequences used for real-time PCR

Genes	Sequence (5' ⟶ 3')	TM(°C)	Accession No	PCR Product length (bp)
Caspase 9	F: GTTTGAGGACCTTCGACCAGCT R: CAACGTACCAGGAGCCACTCTT	62	NM_001229	129
Caspase 3	F: ATGGAAGCGAATCAATGGA R: TGTACCAGACCGAGATGTC	55	NM_001354782.2	137
MMP2	F: TTGACGGTAAGGACGGACTC R: CATACTTCACACGGACCACTTG	59	NM_004994.3	126
MMP9	F: GCACGACGTCTTCCAGTACC R: CAGGATGTCATAGGTCACGTAGC	60	NM_001302510.2	124
β-actin	F: TCCTCCTGAGCGCAAGTAC R: CCTGCTTGCTGATCCACATCT	55	NM_001101.5	89

were analyzed using REST 2009 software based on the comparative ΔΔCt approach, and relative transcript abundance was expressed as $2^{-\Delta\Delta Ct}$. Graphical presentation of gene expression data was prepared using GraphPad Prism 6. Melt curve analysis was performed following amplification to verify the specificity of each PCR product and to exclude nonspecific amplification or primer-dimer formation.

Apoptosis Analysis

Apoptotic cell death was evaluated by Annexin V-FITC/propidium iodide (PI) dual staining followed by flow cytometric analysis. MDA-MB-231 cells were exposed to the IC_{50} concentration of *R. persica*-mediated AgNPs under the same experimental conditions used for the cytotoxicity assay. Following treatment, cells were harvested, stained according to the manufacturer's instructions, and analyzed by flow cytometry. Cell populations were classified into viable, early apoptotic, late apoptotic, and necrotic fractions based on their Annexin V-FITC and PI staining profiles.

Statistical Analysis

All experiments were conducted in three independent replicates, and the results are presented as mean ± standard deviation (SD). Statistical analyses were performed using one-way analysis of variance (ANOVA) followed by Tukey's multiple comparison post hoc test to evaluate differences among experimental groups. Statistical significance was defined as a p value of less than 0.05.

RESULTS

Characterization of Silver Nanoparticles Synthesized from Rhamnus persica Leaf Extract

The green synthesis of silver nanoparticles using *Rhamnus persica* leaf extract was successfully accomplished, as evidenced by the gradual color transition of the reaction mixture from colorless to dark brown within approximately 4 h, indicating the reduction of Ag^+ ions and nanoparticle formation. UV–Visible spectroscopic analysis further verified nanoparticle synthesis by displaying a distinct surface plasmon resonance (SPR) absorption peak at 445 nm.

The crystalline characteristics of the synthesized nanoparticles were examined by X-ray diffraction analysis. The diffraction pattern exhibited prominent reflections at 2θ values of 33°, 35°, 38°, and 48°, confirming the crystalline nature of the AgNPs and their face-centered cubic (fcc) structure.

Morphological evaluation by scanning electron microscopy (SEM) demonstrated that the nanoparticles displayed heterogeneous dimensions ranging from 17.9 to 60.3 nm, with limited particle aggregation observed in some regions. Transmission electron microscopy (TEM) provided additional structural information and showed that most nanoparticles possessed a predominantly spherical morphology with particle diameters reaching approximately 80 nm. Dynamic light scattering (DLS) analysis revealed a major hydrodynamic size distribution between 20 and 30 nm, which differs from electron microscopy measurements because DLS determines the hydrodynamic diameter of particles dispersed in solution rather than the physical core diameter.

Fourier-transform infrared (FTIR) spectroscopy identified characteristic absorption bands corresponding to O–H, C=O, C=C, and C–O functional groups. These findings indicate that naturally occurring biomolecules, particularly phenolic and flavonoid constituents present in the *R. persica* extract, likely participated in both the reduction of silver ions and stabilization of the synthesized nanoparticles (Fig. 1). Although the FTIR spectrum of the crude plant extract was not analyzed separately, the detected functional groups are consistent with those previously reported for phenolic-rich plant extracts employed in green synthesis of metallic nanoparticles.

Cytotoxic Effects of Rhamnus persica-Derived AgNPs and the Free Plant Extract on MDA-MB-231 Cells

The cytotoxic activities of biosynthesized *R. persica* AgNPs and the corresponding free plant extract were evaluated in MDA-MB-231 cells using the MTT assay. Both treatments produced concentration-dependent decreases in cell viability; however, the nanoparticle formulation consistently exhibited substantially greater cytotoxic potency across the entire concentration range examined. At the highest tested concentration (100 µg/mL), treatment with AgNPs reduced cell viability to 23.44 ± 0.45%, whereas exposure to an equivalent concentration of the free extract resulted in 74.65 ± 0.36% viable cells (Fig. 2).

The half-maximal inhibitory concentration (IC_{50}) of the AgNP formulation was calculated to

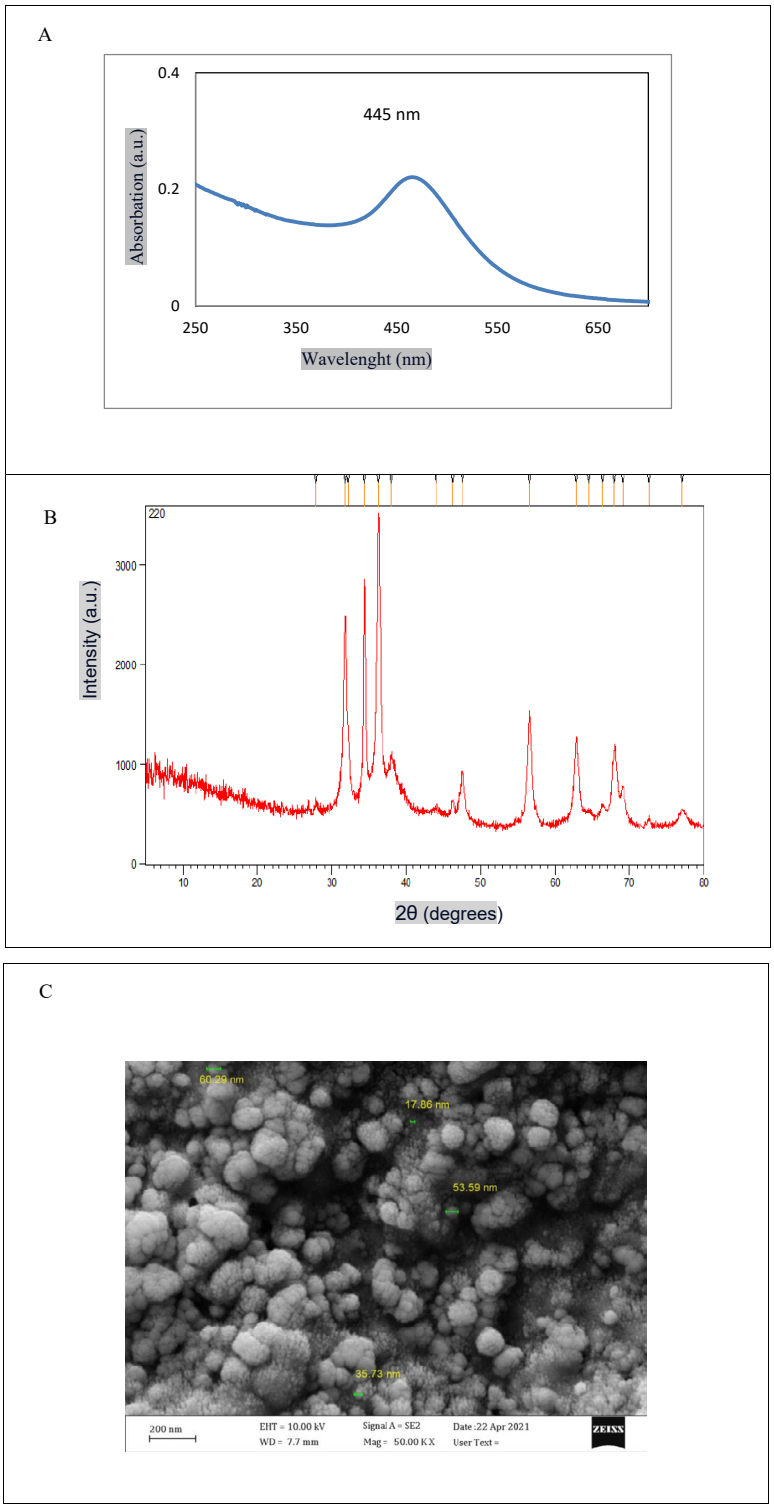

Fig. 1. Physicochemical characterization of biosynthesized *Rhamnus persica*-mediated silver nanoparticles (AgNPs). (A) UV–Visible absorption spectrum demonstrating the characteristic surface plasmon resonance (SPR) peak at 445 nm, confirming nanoparticle formation. (B) X-ray diffraction (XRD) pattern showing the crystalline structure of the synthesized silver nanoparticles. (C) Scanning electron microscopy (SEM) micrographs illustrating nanoparticle morphology together with particle size variation. (D) Transmission electron microscopy (TEM) images demonstrating the predominantly spherical morphology of the AgNPs. (E) Dynamic light scattering (DLS) profile presenting the hydrodynamic particle size distribution and polydispersity in aqueous suspension. (F) Fourier-transform infrared (FTIR) spectrum indicating the major functional groups associated with phytochemicals involved in the reduction and stabilization of the biosynthesized nanoparticles.

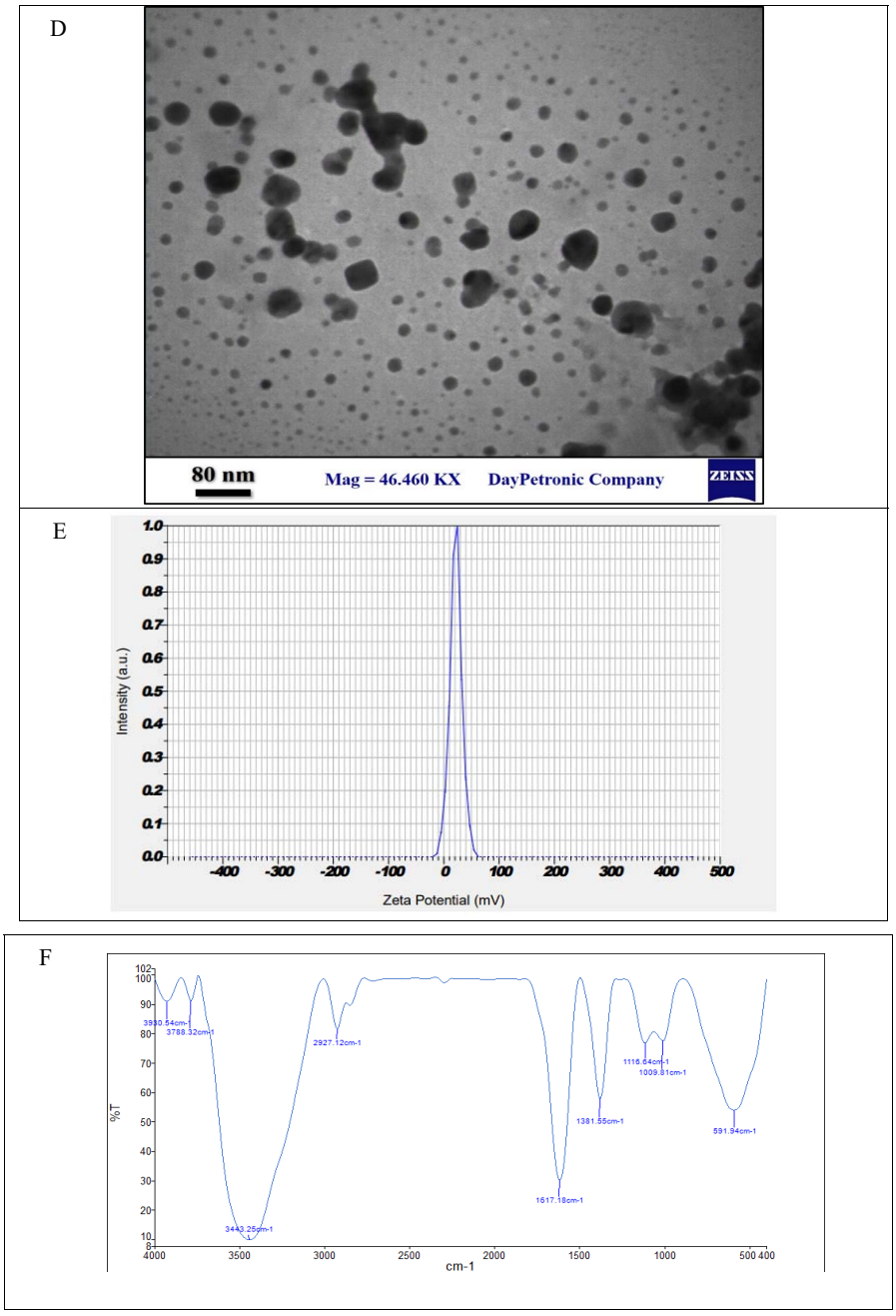

Continued Fig. 1. Physicochemical characterization of biosynthesized *Rhamnus persica*-mediated silver nanoparticles (AgNPs). (A) UV–Visible absorption spectrum demonstrating the characteristic surface plasmon resonance (SPR) peak at 445 nm, confirming nanoparticle formation. (B) X-ray diffraction (XRD) pattern showing the crystalline structure of the synthesized silver nanoparticles. (C) Scanning electron microscopy (SEM) micrographs illustrating nanoparticle morphology together with particle size variation. (D) Transmission electron microscopy (TEM) images demonstrating the predominantly spherical morphology of the AgNPs. (E) Dynamic light scattering (DLS) profile presenting the hydrodynamic particle size distribution and polydispersity in aqueous suspension. (F) Fourier-transform infrared (FTIR) spectrum indicating the major functional groups associated with phytochemicals involved in the reduction and stabilization of the biosynthesized nanoparticles.

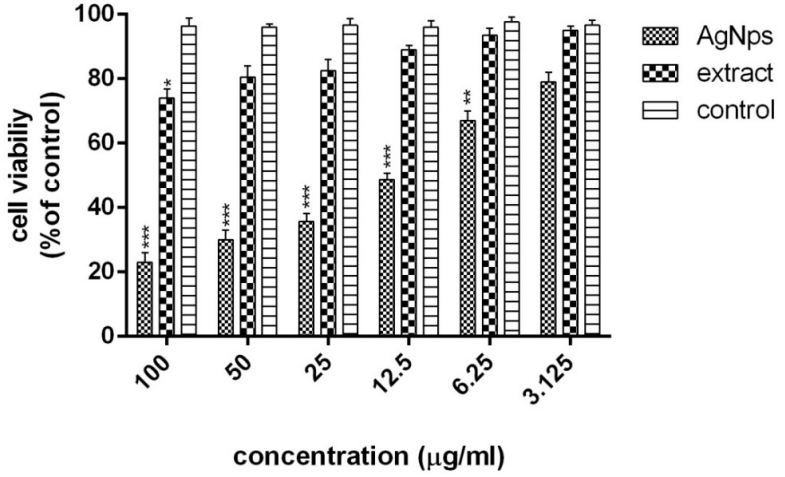

Fig. 2. Concentration-dependent cytotoxic activity of *Rhamnus persica*-mediated silver nanoparticles (AgNPs) and the corresponding free plant extract against MDA-MB-231 cells. Cells were exposed to increasing concentrations (3.125–100 μg/mL) of each treatment for 24 h, and cell viability was determined using the MTT assay. Results are presented as the percentage of viable cells relative to untreated controls (mean ± SD, $n = 3$ independent experiments). Statistical comparisons were performed using one-way ANOVA followed by Tukey's multiple comparison test ($p < 0.05$, $p < 0.01$, $p < 0.001$).

be 9.45 μg/mL, demonstrating markedly greater biological activity than the free extract, which exhibited an IC_{50} of 990.55 μg/mL. This difference remained evident at lower concentrations. For example, treatment with 6.25 μg/mL AgNPs decreased cell viability to 67.44 ± 0.43%, whereas cells exposed to the same concentration of the crude extract maintained a viability of 93.44 ± 0.45%, indicating only minimal cytotoxic activity.

Transcriptional Analysis of Apoptosis-Related and Extracellular Matrix-Associated Genes

The transcriptional responses of apoptosis-related and extracellular matrix-associated genes were evaluated by quantitative real-time PCR following treatment with *R. persica*-mediated AgNPs or the corresponding free extract at their respective IC_{50} concentrations. AgNP treatment significantly increased the expression of the apoptotic genes *Caspase-3* and *Caspase-9* by 3.70 ± 0.87-fold and 3.99 ± 0.89-fold, respectively ($p < 0.001$). In contrast, treatment with the free extract produced smaller, although statistically significant, increases in *Caspase-3* (2.09 ± 0.65-fold) and *Caspase-9* (2.44 ± 0.78-fold) expression.

Expression of the extracellular matrix-associated genes *MMP2* and *MMP9* was reduced in cells treated with the nanoparticle formulation, reaching 0.58 ± 0.26-fold and 0.63 ± 0.19-fold, respectively ($p < 0.01$). The free extract also produced decreases in the expression of these genes; however, the observed changes were not statistically significant (Fig. 3). Because these analyses were limited to mRNA expression, the reductions in *MMP2* and *MMP9* should be interpreted as molecular findings only and should not be considered evidence of altered migratory, invasive, or anti-metastatic activity in the absence of dedicated functional assays.

Flow Cytometric Analysis of Apoptosis

Apoptotic cell death induced by the nanoparticle formulation and the free extract was further evaluated by Annexin V-FITC/PI flow cytometry following treatment at their respective IC_{50} concentrations. Cells exposed to *R. persica*-mediated AgNPs exhibited 14.7% early apoptotic cells and 11.2% late apoptotic cells, corresponding to a total apoptotic population of 25.9%, whereas only 1.39% of cells were classified as necrotic. In comparison, treatment with the free extract resulted in a lower overall apoptotic population (17.19%) together with minimal necrosis (0.47%) (Fig. 4). These findings indicate that nanoparticle formulation enhanced apoptosis induction without a corresponding increase in necrotic cell death, supporting apoptosis as the predominant mechanism underlying the observed reduction in cell viability.

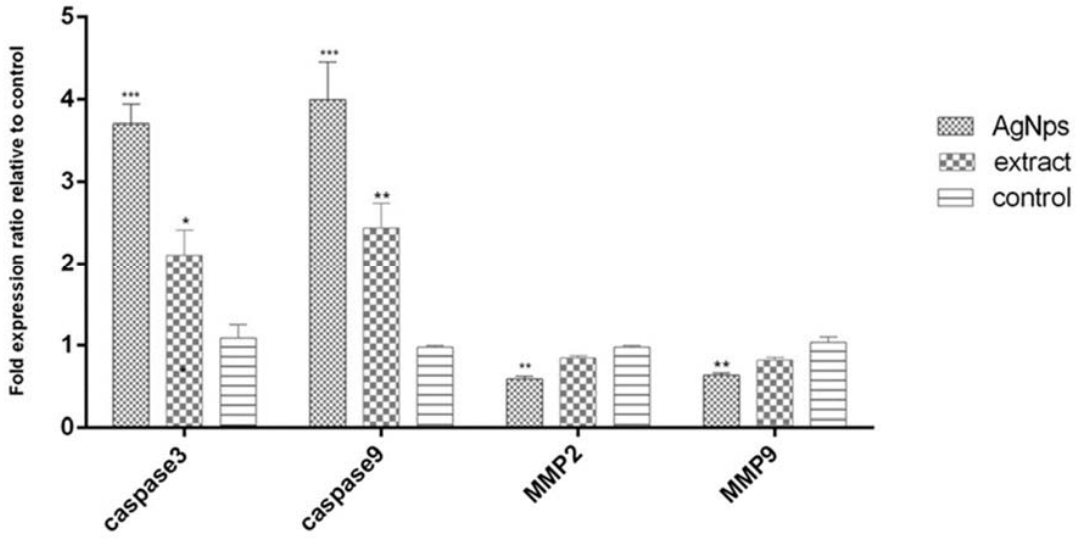

Fig. 3. Relative transcriptional expression of apoptosis-related and extracellular matrix-associated genes in MDA-MB-231 cells following treatment with *Rhamnus persica*-mediated silver nanoparticles (AgNPs) and the corresponding free extract. Messenger RNA levels of *Caspase-3*, *Caspase-9*, *MMP2*, and *MMP9* were determined by quantitative real-time PCR after 24 h of treatment at the respective IC_{50} concentrations. Gene expression values were normalized to β-actin and calculated using the comparative $2^{-\Delta\Delta Ct}$ method. Results are expressed as mean ± SD ($n = 3$ independent experiments). Statistical significance was evaluated by one-way ANOVA ($p < 0.05$, $p < 0.01$, $p < 0.001$).

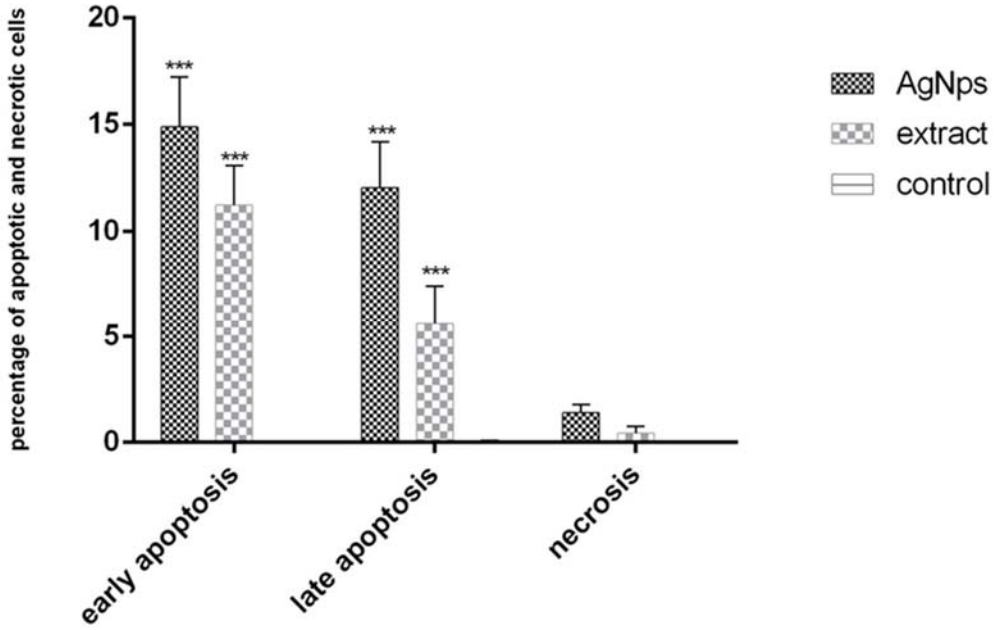

Fig. 4. Flow cytometric evaluation of apoptosis in MDA-MB-231 cells following treatment with *Rhamnus persica*-mediated silver nanoparticles (AgNPs) and the corresponding free extract. Cells were exposed to the respective IC_{50} concentrations for 24 h and subsequently stained with Annexin V-FITC and propidium iodide (PI) before flow cytometric analysis. Representative dot plots together with quantitative data illustrate the distribution of viable, early apoptotic, late apoptotic, and necrotic cell populations. Results are presented as mean ± SD ($n = 3$ independent experiments). Statistical differences among experimental groups were analyzed using one-way ANOVA followed by Tukey's multiple comparison test ($p < 0.05$, $p < 0.01$, $p < 0.001$).

DISCUSSION

Breast cancer continues to represent a major global health challenge and remains one of the principal causes of cancer-related morbidity among women despite substantial progress in screening, diagnosis, and treatment [18]. Consequently, the identification of safer and more effective therapeutic alternatives has become an important focus of current cancer research. Plant-derived bioactive compounds have received considerable attention because of their broad pharmacological properties, including antioxidant, anti-inflammatory, and antiproliferative activities, together with their generally favorable safety profiles [19,20]. Among medicinal plants, *R. persica* has emerged as a promising source of phytochemicals such as flavonoids and phenolic compounds, which are known to participate in the regulation of signaling pathways associated with cancer cell survival and programmed cell death [21,22]. In the present study, the crude *R. persica* leaf extract exhibited measurable cytotoxic activity against MDA-MB-231 cells, whereas its incorporation into biogenic silver nanoparticles substantially enhanced these biological effects. Compared with the free extract, *R. persica*-mediated AgNPs produced markedly lower IC_{50} values and induced a more pronounced apoptotic response, as confirmed by both transcriptional analysis and flow cytometric assessment [23]. These observations are in agreement with previous studies demonstrating that nanoparticle-based delivery systems improve the stability, cellular uptake, intracellular retention, and biological performance of plant-derived bioactive compounds [24,25].

At the molecular level, treatment with *R. persica*-mediated AgNPs resulted in coordinated transcriptional upregulation of the apoptotic regulators *Caspase-3* and *Caspase-9*, accompanied by downregulation of extracellular matrix-associated genes *MMP2* and *MMP9*. Importantly, these findings should be interpreted exclusively at the gene expression level and do not indicate functional alterations in cell migration or invasion. Instead, they provide preliminary molecular evidence regarding pathways that may be influenced by the nanoparticle formulation. The observed transcriptional modulation may be explained by improved intracellular delivery, increased surface reactivity, and sustained release of phytochemicals associated with the nanoscale properties of the AgNPs [26]. Moreover, the flow cytometric findings demonstrated that the enhanced cytotoxicity was predominantly mediated through apoptosis rather than necrosis, suggesting a controlled mode of cell death with potential therapeutic relevance [27]. It should also be emphasized that the reduced expression of *MMP2* and *MMP9* was determined solely at the mRNA level. Because migration, invasion, and extracellular matrix remodeling assays were beyond the scope of the present study, these molecular alterations should not be interpreted as evidence of anti-metastatic or anti-invasive activity. Rather, they identify potential signaling pathways that merit investigation through dedicated functional studies.

Natural-product-based therapeutic strategies possess several advantages over conventional single-target approaches because phytochemicals frequently influence multiple signaling pathways simultaneously, potentially reducing the emergence of therapeutic resistance [13,28,29]. The incorporation of these compounds into nanocarrier systems may further improve their pharmacological performance by enhancing stability, bioavailability, and cellular delivery while permitting lower effective doses and potentially reducing off-target toxicity [30,31]. Collectively, the present findings support the concept that green nanotechnology can substantially improve the biological activity of medicinal plant extracts and strengthen their molecular anticancer effects.

Although the present investigation was restricted to in vitro cytotoxicity, apoptosis, and gene expression analyses, the results provide valuable mechanistic insight into the biological activity of *R. persica*-derived silver nanoparticles against triple-negative breast cancer cells. The enhanced induction of apoptosis together with the transcriptional modulation of extracellular matrix-associated genes suggests that nanoparticle formulation improves the anticancer potential of the plant extract at the molecular level. Nevertheless, because functional migration, invasion, and extracellular matrix remodeling assays were not performed, the observed changes in *MMP2* and *MMP9* expression should be regarded as preliminary molecular findings rather than direct evidence of anti-metastatic efficacy. Future investigations incorporating functional in vitro assays, protein-level validation, and appropriate in vivo models will be necessary to clarify the

therapeutic significance and translational potential of *R. persica*-mediated silver nanoparticles for the treatment of aggressive breast cancer [32].

CONCLUSION

In conclusion, the present study demonstrates that silver nanoparticles biosynthesized using *R.persica* leaf extract exert pronounced cytotoxic effects against triple-negative breast cancer MDA-MB-231 cells and preferentially induce apoptotic cell death. Compared to the free plant extract, the nanoparticle formulation significantly enhanced anticancer activity, as evidenced by lower IC_{50} values, increased apoptotic cell populations, and coordinated upregulation of apoptosis-related genes, including *Caspase-3* and *Caspase-9*.

In addition to apoptotic signaling, treatment with *R. persica*–mediated silver nanoparticles resulted in transcriptional modulation of extracellular matrix–associated genes, namely *MMP2* and *MMP9*. These alterations were evaluated exclusively at the mRNA level and are not indicative of functional changes in cell migration, invasion, or metastatic behavior. Rather, they provide preliminary molecular insight into pathways that may be influenced by the nanoparticle-based formulation.

Overall, this work highlights the potential of integrating phytochemical-rich plant extracts with nanotechnology to enhance cytotoxic and pro-apoptotic responses in aggressive breast cancer models. While the findings are limited to in vitro cytotoxicity, apoptosis profiling, and gene expression analyses, they establish a molecular framework that supports further functional and translational studies to elucidate the biological relevance and therapeutic applicability of *R. persica*–derived silver nanoparticles.

ACKNOWLEDGMENTS

The authors gratefully acknowledge all individuals who provided assistance, guidance, or support during the course of this research.

CONFLICT OF INTEREST

The authors declare no conflict of interest.

REFERENCES

1. Wilkinson L, Gathani T. Understanding breast cancer as a global health concern. Br J Radiol. 2022;95(1130):20211033. https://doi.org/10.1259/bjr.20211033
2. Singal AG, Kanwal F, Llovet JM. Global trends in hepatocellular carcinoma epidemiology: implications for screening, prevention and therapy. Nat Rev Clin Oncol. 2023;20(12):864-884. https://doi.org/10.1038/s41571-023-00825-3
3. Ensenyat-Mendez M, et al. Current triple-negative breast cancer subtypes: dissecting the most aggressive form of breast cancer. Front Oncol. 2021;11:681476. https://doi.org/10.3389/fonc.2021.681476
4. Medina MA, et al. Triple-negative breast cancer: a review of conventional and advanced therapeutic strategies. Int J Environ Res Public Health. 2020;17(6):2078. https://doi.org/10.3390/ijerph17062078
5. Cai WY, et al. DNA methylation and immune evasion in triple-negative breast cancer: challenges and therapeutic opportunities. Front Oncol. 2025;15:1534055. https://doi.org/10.3389/fonc.2025.1534055
6. Dogheim GM, Amralla MT. Proteolysis Targeting Chimera (PROTAC) as a promising novel therapeutic modality for the treatment of triple-negative breast cancer (TNBC). Drug Dev Res. 2023;84(4):629-653. https://doi.org/10.1002/ddr.22055
7. Ashrafi A, et al. Current landscape of therapeutic resistance in lung cancer and promising strategies to overcome resistance. Cancers (Basel). 2022;14(19):4562. https://doi.org/10.3390/cancers14194562
8. Xia X. Drug efficacy and toxicity prediction: an innovative application of transcriptomic data. Cell Biol Toxicol. 2020;36(6):591-602. https://doi.org/10.1007/s10565-020-09552-2
9. Dehelean CA, et al. Plant-derived anticancer compounds as new perspectives in drug discovery and alternative therapy. Molecules. 2021;26(4):1109. https://doi.org/10.3390/molecules26041109
10. Tesfaye S, et al. Ethiopian medicinal plants traditionally used for the treatment of cancer, part 2: A review on cytotoxic, antiproliferative, and antitumor phytochemicals, and future perspective. Molecules. 2020;25(17):4032. https://doi.org/10.3390/molecules25174032
11. Mitra T, Bhattacharya R. Phytochemicals modulate cancer aggressiveness: A review depicting the anticancer efficacy of dietary polyphenols and their combinations. J Cell Physiol. 2020;235(11):7696-7708. https://doi.org/10.1002/jcp.29703
12. Ogunlakin AD, et al. Medicinal Plants and Phytochemicals Targeting Specific Cancer Pathways and Mechanisms. In: Medicinal Plants and Their Bioactives in Human Diseases. Springer; 2025. p. 235-257. https://doi.org/10.1007/978-3-032-01356-9_11
13. Zhao W, et al. Advances of antitumor drug discovery in traditional Chinese medicine and natural active products by using multi-active components combination. Med Res Rev. 2023;43(5):1778-1808. https://doi.org/10.1002/med.21963
14. Akram M, et al. Herbal medicine for the management of laxative activity. Curr Pharm Biotechnol. 2022;23(10):1269-1283. https://doi.org/10.2174/1389201022666210812121328
15. Nwozo OS, et al. Antioxidant, phytochemical, and therapeutic properties of medicinal plants: A review. Int J Food Prop. 2023;26(1):359-388. https://doi.org/10.1080/10942912.2022.2157425
16. Huang S, et al. The role and mechanism of Perilla frutescens in cancer treatment. Molecules. 2023;28(15):5883. https://doi.org/10.3390/molecules28155883
17. Albahri G, et al. Potential anti-tumorigenic properties of diverse medicinal plants against the majority of common

types of cancer. Pharmaceuticals (Basel). 2024;17(5):574. https://doi.org/10.3390/ph17050574
18. Cuthrell KM, Tzenios N. Breast cancer: updated and deep insights. Int Res J Oncol. 2023;6(1):104-118.
19. Kangra K, et al. Incredible use of plant-derived bioactives as anticancer agents. RSC Adv. 2025;15(3):1721-1746. https://doi.org/10.1039/D4RA05089D
20. Homaeii S, Kavousi M, Asgari EA. Investigating the apoptotic and antimetastatic effect of daphnetin-containing nano niosomes on MCF-7 cells. Adv Cancer Biol Metastasis. 2025;14:100139. https://doi.org/10.1016/j.adcanc.2025.100139
21. Asadi P, et al. Content of saponin, tannin, and flavonoid in the leaves and fruits of Iranian populations from Rhamnus persica Boiss. (Rhamnaceae). Int J Second Metab. 2024;11(2):235-243. https://doi.org/10.21448/ijsm.1391683
22. Chavda VP, et al. Advanced phytochemical-based nanocarrier systems for the treatment of breast cancer. Cancers (Basel). 2023;15(4):1023. https://doi.org/10.3390/cancers15041023
23. Le TTH, et al. Anti-cancer activity of green synthesized silver nanoparticles using Ardisia gigantifolia leaf extract against gastric cancer cells. Biochem Biophys Res Commun. 2023;661:99-107. https://doi.org/10.1016/j.bbrc.2023.04.037
24. Iqubal MK, et al. Targeted delivery of natural bioactives and lipid-nanocargos against signaling pathways involved in skin cancer. Curr Med Chem. 2021;28(39):8003-8035. https://doi.org/10.2174/0929867327666201104151752
25. Abdel-Hamid NM, Abass SA. Matrix metalloproteinase contribution in management of cancer proliferation, metastasis and drug targeting. Mol Biol Rep. 2021;48(9):6525-6538. https://doi.org/10.1007/s11033-021-06635-z
26. Upaganlawar A, et al. Effective cancer management: Inimitable role of phytochemical based nano-formulations. Curr Drug Metab. 2022;23(11):869-881. https://doi.org/10.2174/1389200223666220905162245
27. Bozzuto G, et al. Phytocompounds and nanoformulations for anticancer therapy: A review. Molecules. 2024;29(16):3784. https://doi.org/10.3390/molecules29163784
28. Pandey A, Karmous I. Exploring the Potential of Plant-Based Nanotechnology in Cancer Immunotherapy: Benefits, Limitations, and Future Perspectives. Biol Trace Elem Res. 2025;203(3):1746-1763. https://doi.org/10.1007/s12011-024-04266-6
29. Makhoba XH, et al. Potential impact of the multi-target drug approach in the treatment of some complex diseases. Drug Des Devel Ther. 2020;14:3235-3249. https://doi.org/10.2147/DDDT.S257494
30. Li X, et al. Multifunctional nanoparticle-mediated combining therapy for human diseases. Signal Transduct Target Ther. 2024;9(1):1. https://doi.org/10.1038/s41392-023-01668-1
31. Yetisgin AA, et al. Therapeutic nanoparticles and their targeted delivery applications. Molecules. 2020;25(9):2193. https://doi.org/10.3390/molecules25092193
32. Puri A, et al. Plant-derived selenium nanoparticles: investigating unique morphologies, enhancing therapeutic uses, and leading the way in tailored medical treatments. Mater Adv. 2024;5(9):3602-3628. https://doi.org/10.1039/D3MA01126G